



Diagnostic performances of FDG-PET/CT and diffusion-weighted imaging indices for differentiating benign pheochromocytoma from other benign adrenal tumors

Masatoyo Nakajo,¹ Masayuki Nakajo,^{1,2} Yoshihiko Fukukura,¹ Megumi Jinguji,¹ Toshikazu Shindo,¹ Yoshiaki Nakabeppu,¹ Kiyohisa Kamimura,¹ Tomohide Yoneyama,¹ Koji Takumi,¹ Takashi Yoshiura¹

¹Department of Radiology, Graduate School of Medical and Dental Sciences, Kagoshima University, 8-35-1 Sakuragaoka, Kagoshima 890-8544, Japan

²Department of Radiology, Nanpuh Hospital, 14-3 Nagata, Kagoshima 892-8512, Japan

Abstract

Purpose: The purpose of this study is to compare diagnostic performances of ¹⁸F-fluorodeoxyglucose (FDG) visual score, maximum standardized uptake value (SUVmax), ratio of adrenal SUVmax to liver SUVmax (A/L SUVmax), apparent diffusion coefficient (ADC) from diffusion-weighted imaging, and SUVmax/ADC ratio to differentiate adrenal pheochromocytoma from other benign tumors.

Methods: Eleven pheochromocytomas and 22 other benign tumors in 30 patients were included. FDG-based indices, ADC, and SUVmax/ADC ratio were compared between groups using the Mann–Whitney U test, and sensitivity, specificity, accuracy, and area under the curve (AUC) for diagnosing pheochromocytoma by receiver operating characteristic analyses. The correlation between SUVmax and ADC was analyzed using the Spearman's rank test.

Results: Pheochromocytoma showed significantly higher visual score (2.8 ± 0.4 vs. 1.3 ± 0.9), SUVmax (11.0 ± 8.9 vs. 3.2 ± 1.4), A/L SUVmax ratio (3.96 ± 3.48 vs. 0.96 ± 0.51), and SUVmax/ADC ratio (10.6 ± 8.09 vs. 2.28 ± 0.98) (each $P < 0.001$) and significantly lower ADC ($1.08 \pm 0.23 \times 10^{-3} \text{ mm}^2/\text{s}$ vs. $1.43 \pm 0.29 \times 10^{-3} \text{ mm}^2/\text{s}$, $P = 0.003$) than other benign tumors. Sensitivity, specificity, and accuracy for diagnosing pheochromocytoma were 100, 73, and 82%

for visual score, 100, 86, and 91% for both SUVmax and A/L SUVmax ratio, and 64, 100, and 88% for ADC and 82, 95, and 91% for SUVmax/ADC ratio. No significant differences in AUC were found between FDG-based indices, ADC, and SUVmax/ADC ratio. A significant negative correlation was noted between SUVmax and ADC ($\rho = -0.36$, $P = 0.039$).

Conclusion: FDG-based indices and ADC appear comparably useful for differentiating pheochromocytoma from other benign adrenal tumors.

Key words: Adrenal tumor—Pheochromocytoma—FDG—SUV—ADC

The prevalence of adrenal masses incidentally detected by cross-sectional imaging modalities (incidentalomas) may range between 0.35% and 6% of the different imaged population [1, 2]. Although most such adrenal incidentalomas are benign tumors such as adenoma (50–80%) or myelolipoma (5–10%), pheochromocytoma is sometimes discovered incidentally (5%) [1]. The most common clinical conundrum lies in differentiating malignant from benign tumors. However, differentiating pheochromocytoma from other benign adrenal tumors is also important, because management strategies differ substantially.

Imaging plays a key role in the characterization of adrenal tumors. An attenuation value of ≤ 10 Hounsfield unit (HU) on unenhanced computed tomography (CT) is highly specific for lipid-rich adenoma [3]. However, up to 30% of adenomas exhibit attenuation values > 10 HU

(lipid-poor adenomas) and cannot be specifically diagnosed on unenhanced CT [4]. In such cases, other imaging techniques are required for further characterization of the adrenal tumors. Several CT washout percentage methods reportedly offer high diagnostic accuracy for discriminating between adenomas and non-adenomas [1]. Pheochromocytomas not only may show low loss of CT contrast enhancement when compared with adenomas [5], but may also show adenoma-like patterns of enhancement loss [6]. Chemical shift magnetic resonance imaging (MRI) is also useful in differentiating adenomas from non-adenomas [7]. However, some lipid-poor adenomas cannot be differentiated from other adrenal tumors using this technique [1]. Although ^{123}I meta-iodobenzylguanidine (MIBG) imaging is the technique of choice for evaluating pheochromocytoma, offering a specificity of 95–100%, and a sensitivity of 83–100% [8], pheochromocytoma occasionally exhibit variable imaging features that may mimic other benign and malignant tumors.

Uptake of the glucose analog ^{18}F -fluorodeoxyglucose (FDG) represents local glycolytic activity, and this substance has thus seen wide use as a tracer for positron emission tomography (PET)/CT in oncology [9]. FDG-PET has been used for evaluating adrenal lesions, and benign adrenal tumors typically show lower FDG uptake than background liver uptake [10]. Most pheochromocytomas are seen as FDG-avid tumors [11, 12], and FDG-PET may therefore be useful to differentiate pheochromocytoma from other benign adrenal tumors. However, to the best of our knowledge, no reports have focused on this theme.

Diffusion-weighted imaging (DWI) has emerged as a new diagnostic technique in the evaluation of various abdominal lesions and has been shown to be helpful in the characterization of tumors on the basis of water molecular diffusivity through the measurement of apparent diffusion coefficient (ADC) [13]. Despite previous investigational efforts, the usefulness of DWI in characterizing adrenal tumors has not been established [14–18]. In particular, only a few reports have described DWI for pheochromocytoma [18, 19], and the value of this modality in differentiating between pheochromocytoma and other benign adrenal tumors is largely unknown.

Although both FDG-PET and DWI are available for investigating the biological characteristics of tumors, no reports appear to have determined FDG standardized uptake value (SUV) and ADC from DWI in the same patients with adrenal tumors. The aim of this study was to compare the diagnostic performances of FDG-PET/CT-based indices and ADC in differentiating between pheochromocytoma and other benign adrenal tumors.

Materials and methods

Patients

All study protocols for this retrospective study were approved by the institutional review board, and the need to obtain informed consent was waived. From January 2011 to June 2013, a total of 66 consecutive patients underwent MRI for evaluation of suspected adrenal disease. Clinical records were reviewed to identify patients for analysis in the study. Inclusion criteria were (1) patients who underwent both DWI and FDG-PET/CT; (2) with adrenal lesions >1 cm in diameter; and (3) diagnoses confirmed by hormonal, pathological, and/or follow-up imaging examinations.

Final diagnoses of the adrenal tumors were based on the available clinical, imaging, and pathological data. For the definite diagnosis of adenoma when pathological diagnosis was not available, we used imaging results from follow-up for ≥ 6 months. Lesions that showed stability on a 6-month follow-up scan were considered as benign in accordance with a previous report [20]. Adrenal myelolipoma was diagnosed based on the detection of macroscopic fat on CT [21] or surgical pathology. Pheochromocytoma and schwannoma were diagnosed based on surgical pathology.

Imaging protocols

FDG-PET/CT protocols and I-123 MIBG imaging. All PET/CT studies were performed using a Discovery 600 M PET/CT system (GE Medical Systems, Milwaukee, WI). All patients were instructed to fast for ≥ 5 h before the examinations. Image acquisition started 1 h after intravenous injection of FDG (140–210 MBq). At FDG injection, the mean plasma glucose level was 105 mg/dl (range 74–149 mg/dl). CT covering from the brain to the feet was performed immediately before PET using a 16-slice CT scanner [slice thickness, 3.75 mm; pitch, 1.75 mm; 120 keV; auto mA (35–100 mA depending on the total body mass of the patient)]. Whole-body PET was then performed, covering an area identical to that covered by CT. Acquisition time was 2.5 min per bed position, with 14 bed positions. Emission data were reconstructed using a 3-dimensional (3D) ordered-subset expectation maximization algorithm (16 subsets, 2 iterations: VUE Point Plus) to 192×192 matrices using the CT data for attenuation correction. The reconstructed transaxial spatial resolution for PET was 5.1 mm full-width half-maximum in-plane.

^{123}I -MIBG imaging was performed as follows: Anterior and posterior whole-body planar images were acquired 24 h after intravenous injection of 111 MBq of ^{123}I -MIBG, and single photon emission CT (SPECT) was also performed to cover the areas suspected of

abnormal tracer uptake in whole-body planar images (E.COM Signature; Toshiba/Siemens, Tokyo, Japan).

MRI protocols

All MRI studies were performed using a 3.0-T system (Ingenia 3.0 T; Philips Healthcare, Best, the Netherlands) with a maximum gradient strength of 45 mT/m, slew rate of 200 mT/m/s, and a dStream Torso coil. Free breathing DWI with b values of 0 and 1000 s/mm² (motion probing gradients in the x, y, and z directions) was performed in 20 axial slices using a single-shot echo-planar (EP) sequence and spectral presaturation with inversion recovery for fat suppression. Pulse sequence parameters were as follows: repetition time (TR), 5350 ms; echo time (TE), 50 ms; field of view (FOV), 350 mm; matrix, 152 × 112; EP imaging factor, 83; half scan factor, 0.6; sensitivity encoding (SENSE) acceleration factor, 2; section thickness, 5 mm; section gap, 0.5 mm; and number of excitations (NEX), 3. ADC maps were generated using the software supplied with the MRI unit. Prior to DWI, breath-holding transverse fast field-echo in-phase (IP) and opposed-phase (OP) T1-weighted imaging [TR, 150 ms; TE, 2.3 ms (IP) and 1.13 ms (OP); FOV, 350 mm; matrix, 225 × 220; SENSE factor, 1.4; slice thickness, 5 mm; slice gap, 0.5 mm; NEX, 1] and respiratory-triggered transverse T2-weighted turbo spin-echo with fat-suppression imaging [TR, depending on respiratory interval; TE, 73 ms; FOV, 350 mm; matrix, 198 × 256; echo train length, 17; SENSE factor, 2; slice thickness, 5 mm; slice gap, 0.5 mm; NEX, 1] were performed.

Image analysis

All PET/CT images were analyzed on a workstation (Advantage Windows Workstation; GE Healthcare, Milwaukee, WI). Two nuclear medicine radiologists (M.J. and Y.N., with 4 and 2 years of experience in PET/CT interpretation, respectively) who knew the purpose of PET/CT studies but were blinded to clinical and pathological information and results of other imaging studies, interpreted PET/CT images in consensus. They visually scored FDG uptake of a lesion using a 4-point scale [20]: 0, less than the liver; 1, equal to the liver; 2, moderately increased compared to the liver; or 3, markedly increased compared to the liver. In addition, semiquantitative analysis of adrenal tumors was performed by them in consensus using maximum SUV (SUVmax). SUVmax was automatically measured as follows: first, a rectangular 3D-search region of interest (ROI) was drawn around the tumor in a suitable reference transaxial plane, excluding adjacent avid normal structures. The volume of interest was then defined by adapting an orthogonal

ROI in the sagittal plane to encompass the craniocaudal extent of the tumor and in the coronal plane to cover the mediolateral extent of the tumor. A circular ROI measuring 17.5 cm² was placed over the central solid portion of the right hepatic lobe to obtain liver SUVmax. For each lesion, the ratio of adrenal lesion-to-liver SUVmax (A/L SUVmax ratio) was calculated by dividing the adrenal lesion SUVmax by the liver SUVmax.

All images from DWI were reviewed in consensus by two radiologists (T.S. and Y.F., with 12 and 22 years of experience in abdominal radiology, respectively) who were blinded to the clinical and pathological information and results of other imaging studies. ADC distribution was demonstrated on an ADC map using the communication system workstation monitor (SYNAPS; Fujifilm Medical Systems, Tokyo, Japan). Mean ADC was measured within a circular or ovoid ROI placed in each tumor. The size of the ROI was determined to be as large as possible, and care was taken to avoid any cystic, necrotic, or hemorrhagic components using other MRI sequences as reference. The SUVmax/ADC (SUVmax × 10⁻³ mm²/sec ÷ ADC) ratio was a newly generated index using adrenal lesion SUVmax and ADC for discriminating between pheochromocytoma and other benign adrenal tumors or lipid-poor adenomas.

CT attenuation and the size (maximum diameter) of each lesion were measured in consensus by other two radiologists (MT.N. and MY.N., with 13 and 41 years of experience in radiology, respectively) on unenhanced CT from PET/CT. Mean CT density was obtained within a circular or ovoid ROI placed in each tumor, avoiding any cystic, necrotic, hemorrhagic, and macroscopic fatty components. These two radiologists also determined in consensus whether ¹²³I-MIBG uptake was seen in the adrenal tumors.

Statistical analysis

The Mann–Whitney U test was used to assess differences in numerical variables between pheochromocytoma and other benign adrenal tumors. The correlation between SUVmax and ADC was analyzed using the Spearman's rank test. To examine the diagnostic performances of FDG visual score, SUVmax, A/L SUVmax ratio, ADC, and SUVmax/ADC ratio in discriminating between pheochromocytoma and other benign adrenal tumors or lipid-poor adenomas, receiver operating characteristic (ROC) analyses were conducted. Area under the curve (AUC) was compared using the Student's *t* test. Data are expressed as mean value ± standard deviation (SD) and/or range. A value of *P* < 0.05 was considered statistically significant and all *P*-values presented are two-sided. All statistical analyses were performed using MedCalc statistical software (MedCalc Software, Mariakerke, Belgium).

Results

Tumor characteristics

From the initial 66 patients, 35 patients were excluded because only DWI had been performed. One patient with a clinically diagnosed metastatic adrenal tumor from rectal cancer was excluded. Finally, 30 patients (19 males, 11 females; mean (\pm SD) age, 57 ± 20 years; range 16–86 years) with 33 adrenal tumors met the inclusion criteria and thus were eligible for analysis (Fig. 1). Table 1 shows the characteristics of the study population. A unilateral adrenal tumor was present in 27 patients. One patient showed an adenoma in the left adrenal and a pheochromocytoma in the right adrenal. Another patient had a schwannoma in the right gland and a pheochromocytoma in the left gland. The remaining patient showed bilateral pheochromocytomas. As a result, 17 lipid-poor adenomas, 3 myelolipomas, 2 schwannomas, and 11 pheochromocytomas were identified. Fifteen lipid-poor adenomas were diagnosed by lack of both adrenal hyper-function and tumor enlargement

on follow-up CT or MRI studies (mean follow-up period, 272 ± 47 days; range 195–350 days), and two adenomas were diagnosed by surgical pathology. Two myelolipomas were diagnosed by CT and one myelolipoma was diagnosed by surgical pathology. The mean interval between FDG-PET/CT and MRI studies was 25 ± 21 days (range 3–71 days), and 23 patients underwent FDG-PET/CT first.

Unenhanced CT attenuation was >10 HU in all 33 tumors (mean 31.4 ± 7.1 HU; range 20–46 HU), and no significant difference in CT density was seen between pheochromocytoma ($n = 11$; 34.3 ± 7.9 HU; range 22–46 HU) and other benign adrenal tumors ($n = 22$; 29.9 ± 6.3 HU; range 20–39 HU; $P = 0.08$). Pheochromocytoma ($n = 11$; 56 ± 32 mm; range 20–130 mm) was significantly larger than both other benign adrenal tumors ($n = 22$; 30 ± 27 mm; range 12–130 mm; $P = 0.005$) and lipid-poor adenoma ($n = 17$; 20 ± 8 mm; range 12–45 mm; $P < 0.001$).

^{123}I -MIBG imaging was performed in 25 patients with 28 adrenal tumors. All 11 pheochromocytomas

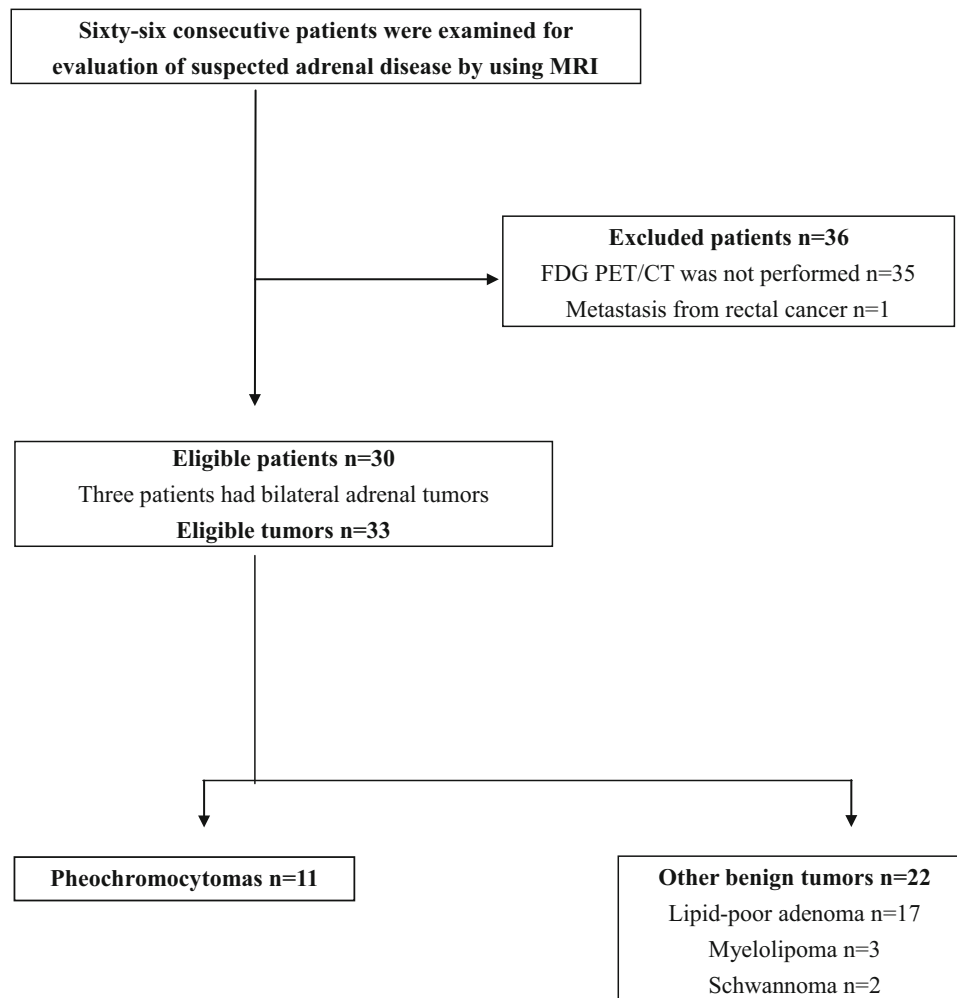


Fig. 1. Flow-chart of the study population.

Table 1. Characteristics of 33 adrenal tumors in 30 patients

Case number	Sex	Age	Tumor number	Diagnosis	Side	Size (mm)	CT density (HU)	I-123 MIBG	FDG-PET		ADC ($\times 10^{-3}$ mm ² /s)	SUVmax/ADC ratio ^b
									Score	SUVmax		
1	M	65	1	Adenoma	L	17	30	Negative	0	2.1	1.96	1.07
2	M	64	2	Adenoma	L	12	25	NP	1	3.2	1.10	2.91
3	M	63	3	Adenoma	L	45	23	Negative	1	2.9	1.92	1.51
4	M	53	4	Adenoma	R	20	22	Negative	0	2.1	1.29	1.63
5	M	27	5	Adenoma	L	12	39	Negative	1	2.6	1.22	2.13
6	M	62	6	Adenoma	L	22	22	Negative	1	3.3	1.23	2.68
7	M	64	7	Adenoma	R	15	32	NP	1	2.9	1.99	1.46
8	F	44	8	Adenoma	L	15	26	Negative	1	2.2	1.13	1.95
9	M	84	9	Adenoma	R	12	20	Negative	1	2.8	1.59	1.76
10	F	76	10	Adenoma	L	27	34	Negative	0	1.9	1.14	1.67
11	M	72	11	Adenoma	L	16	35	Negative	1	2.5	1.18	2.11
12	F	46	12	Adenoma	L	26	38	NP	1	2.7	1.34	2.01
13	M	72	13	Adenoma	L	26	27	Negative	1	2.4	1.49	1.61
14	M	46	14	Adenoma	L	25	36	Negative	1	2.4	1.28	1.88
15	M	63	15	Adenoma	R	27	34	Negative	2	3.2	1.46	2.19
16	F	60	16	Adenoma	L	15	34	Negative	2	2.9	1.29	2.25
17	F	52	17	Adenoma	L	22	32	Negative	2	3	1.71	1.75
18	M	66	18	Myelolipoma	L	50	37	NP	1	2.8	1.18	2.37
19	M	55	19	Myelolipoma	L	30	36	Negative	3	7.9	1.40	5.64
20	F	65	20	Myelolipoma	L	20	20	NP	1	3.0	1.19	2.52
21	M	81	21	Schwannoma	R	130	23	Negative	3	5.8	1.45	4
22	F	69	22	Schwannoma	R	85	33	Negative	3	5.7	1.92	2.97
23	M	27	23	Pheochromocytoma	R	20	37	Positive	3	6.4	0.79	8.1
24	M	81	24	Pheochromocytoma	L	80	28	Positive	3	6	1.07	5.61
25	M	30	25	Pheochromocytoma	L	130	25	Positive	3	32.5	1.43	22.7
26	M	16	26	Pheochromocytoma	R	55	36	Positive	3	12.1	1.08	11.2
27	F	86	27	Pheochromocytoma	L	30	27	Positive	3	18.9	0.96	19.7
28	F	72	28	Pheochromocytoma	L	40	22	Positive	2	4	1.23	3.25
29	F	84	29	Pheochromocytoma	R	50	38	Positive	3	6.1	0.95	6.42
30	F	31	30	Pheochromocytoma	R	20	44	Positive	3	7.9	1.01	7.82
28	F	31	31	Pheochromocytoma	R	75	46	Positive	3	18.1	0.72	25.1
29	M	37	32	Pheochromocytoma	L	70	35	Positive	2	3.8	1.40	2.71
30	M	50	33	Pheochromocytoma	R	46	38	Positive	3	5.1	1.26	4.05

SUVmax, maximum standardized uptake value; ADC, apparent diffusion coefficient; L, left; R, right; CT HU, CT Hounsfield unit; NP, not performed

^a A/L SUVmax ratio = adrenal lesion-to-liver SUVmax ratio

^b SUVmax/ADC ratio = adrenal lesion SUVmax $\times 10^{-3}$ mm²/s/ADC

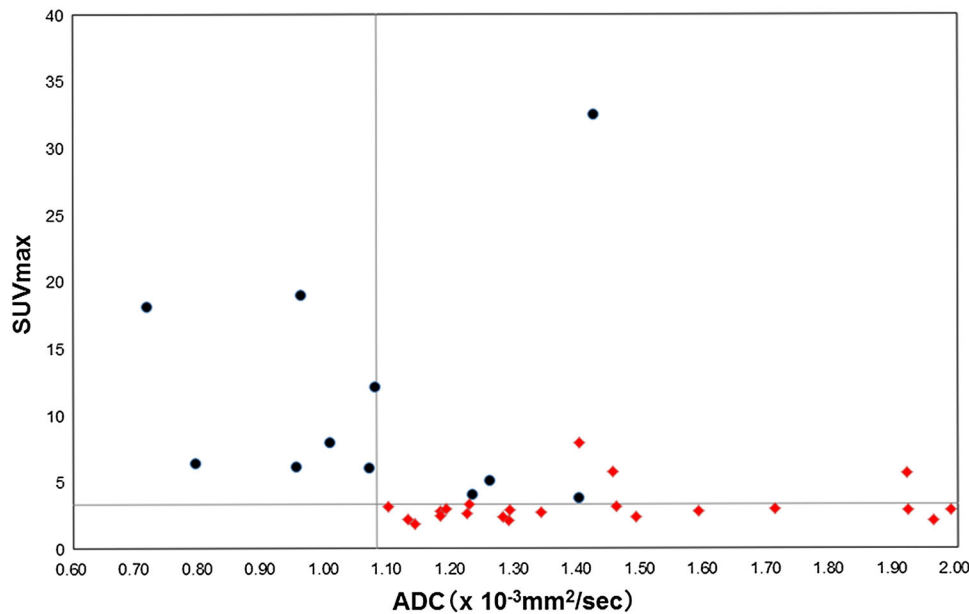


Fig. 2. Scatter plots of primary tumor FDG SUVmax and ADC in 33 adrenal tumors. A significant negative correlation is seen between SUVmax and ADC ($\rho = -0.36$, $P = 0.039$). *Filled circle*: Pheochromocytoma; *filled diamond*: Other benign

adrenal tumor. The horizontal line at an SUVmax of 3.3 and the vertical line at an ADC of $1.08 \times 10^{-3} \text{ mm}^2/\text{s}$ represent the optimum thresholds to discriminate between pheochromocytoma and other benign adrenal tumor groups, respectively.

showed avid (positive) uptake, and all other 17 benign tumors showed non-avid (negative) uptake on ^{123}I -MIBG imaging. The interval between ^{123}I -MIBG imaging and FDG-PET/CT or MRI was 16 ± 9 days (range 1–31 days), and 15 patients underwent ^{123}I -MIBG imaging first.

Comparison of FDG indices and ADC between pheochromocytoma and other benign adrenal tumors

All FDG indices were significantly higher, and ADC was significantly lower in pheochromocytoma ($n = 11$) than in other benign tumors ($n = 22$). Mean values for pheochromocytoma and other benign tumors were 2.8 ± 0.4 (range 2–3) vs. 1.3 ± 0.9 (range 0–3) for visual score ($P < 0.001$), 11.0 ± 8.9 (range 3.8–32.5) vs. 3.2 ± 1.4 (range 1.9–7.9) for SUVmax ($P < 0.001$), 3.96 ± 3.48 (range 1.1–10.8) vs. 0.96 ± 0.51 (range 0.58–2.59) for A/L SUVmax ratio ($P < 0.001$), and $1.08 \pm 0.23 \times 10^{-3} \text{ mm}^2/\text{s}$ (range $0.72\text{--}1.43 \times 10^{-3} \text{ mm}^2/\text{s}$) vs. $1.43 \pm 0.29 \times 10^{-3} \text{ mm}^2/\text{s}$ (range $1.10\text{--}1.99 \times 10^{-3} \text{ mm}^2/\text{s}$) for ADC ($P = 0.003$), respectively. All FDG indices were also significantly higher, and ADC was significantly lower in pheochromocytoma ($n = 11$) than in lipid-poor adenoma ($n = 17$). Mean values for lipid-poor adenoma were 1.0 ± 0.6 (range 0–2) for visual score ($P < 0.001$ compared with pheochromocytoma), 2.7 ± 0.4 (range 1.9–3.3) for SUVmax ($P < 0.001$), 0.78 ± 0.14 (range 0.58–1.00) for A/L SUVmax ratio ($P < 0.001$), and $1.43 \pm 0.30 \times 10^{-3} \text{ mm}^2/\text{s}$ (range

$1.10\text{--}1.99 \times 10^{-3} \text{ mm}^2/\text{s}$) for ADC ($P = 0.004$), respectively. SUVmax/ADC ratio was also significantly higher in pheochromocytoma (mean 10.6 ± 8.09 ; range 2.71–25.1) than in other benign tumors (mean 2.28 ± 0.98 ; range 1.07–5.64) or lipid-poor adenoma (mean 1.91 ± 0.45 ; range 1.07–2.91) (both $P < 0.001$). SUVmax and ADC showed a significant negative correlation ($\rho = -0.36$, $P = 0.039$) (Fig. 2).

FDG indices and ADC to differentiate pheochromocytoma from other benign adrenal tumors

Optimal cutoff values were 2 for visual score, 3.3 for SUVmax, 1.0 for A/L SUVmax ratio, $1.08 \times 10^{-3} \text{ mm}^2/\text{s}$ for ADC, and 4.0 for SUVmax/ADC ratio to differentiate between pheochromocytoma and other benign adrenal tumors. Diagnostic performances of the FDG indices and ADC to detect pheochromocytoma are summarized in Table 2. Accuracy and AUC were 82% and 0.91 for visual score, 91% and 0.95 for SUVmax, 91% and 0.93 for A/L SUVmax ratio, 88% and 0.83 for ADC, and 91% and 0.97 for SUVmax/ADC ratio. No significant differences in AUC were found among FDG indices, ADC and SUVmax/ADC ratio ($P \geq 0.05$ each).

The accuracies of the combined diagnosis of two of FDG-PET indices, ADC and SUVmax/ADC ratio, were not superior to the individual index in differentiating pheochromocytomas from other benign tumors as shown in Table 3.

Table 2. Diagnostic performances of FDG-based indices and ADC for diagnosing pheochromocytoma

Index	Threshold value criterion	Sensitivity (%)	Specificity (%)	Accuracy (%)	AUC
Visual score	≥2	100 (11/11) 72–100 ^a	73 (16/22) 50–89 ^a	82(27/33) 65–93 ^a	0.91 0.75–0.98 ^a
SUVmax	> 3.3	100 (11/11) 72–100 ^a	86 (19/22) 65–97 ^a	91 (30/33) 76–98 ^a	0.95 0.81–0.99 ^a
A/L SUVmax ratio ^b	> 1.0	100 (11/11) 72–100 ^a	86 (19/22) 65–97 ^a	91 (30/33) 76–98 ^a	0.93 0.78–0.99 ^a
ADC	≤1.08	64 (7/11) 31–89 ^a	100 (22/22) 85–100 ^a	88 (29/33) 72–97 ^a	0.83 0.66–0.94 ^a
SUVmax/ADC ratio ^c	>4.0	82 (9/11) 48–98 ^a	95 (21/22) 77–99 ^a	91 (30/33) 76–98 ^a	0.97 0.84–0.99 ^a

SUVmax, maximum standardized uptake value; ADC, apparent diffusion coefficient (10^{-3} mm²/s); AUC, area under the ROC curve

^a 95% confidence interval

^b A/L SUVmax ratio = adrenal lesion-to-liver SUVmax ratio

^c SUVmax/ADC ratio = adrenal lesion SUVmax $\times 10^{-3}$ mm²/s/ADC

Table 3. Diagnostic performances for diagnosing pheochromocytoma using combined use of two indices

Combined criterion	Sensitivity (%)	Specificity (%)	Accuracy (%)
One index and another index			
Visual score ≥ 2 and ADC ≤ 1.08	64(7/11) 31–89 ^a	73 (16/22) 50–89 ^a	70 (23/33) 51–84 ^a
SUVmax > 3.3 and ADC ≤ 1.08	64(7/11) 31–89 ^a	86 (19/22) 65–97 ^a	79 (26/33) 61–91 ^a
A/L SUVmax ratio ^b > 1.0 and ADC ≤ 1.08	64(7/11) 31–89 ^a	86 (19/22) 65–97 ^a	79 (26/33) 61–91 ^a
Visual score ≥ 2 and SUVmax/ADC ratio ^c > 4.0	82(9/11) 48–98 ^a	73 (16/22) 50–89 ^a	76 (25/33) 51–84 ^a
SUVmax > 3.3 and SUVmax/ADC ratio ^c > 4.0	82(9/11) 48–98 ^a	86 (19/22) 65–97 ^a	85 (28/33) 61–91 ^a
A/L SUVmax ratio ^b > 1.0 and SUVmax/ADC ratio ^c > 4.0	82(9/11) 48–98 ^a	86 (19/22) 65–97 ^a	85 (28/33) 61–91 ^a
ADC ≤ 1.08 and SUVmax/ADC ratio ^c > 4.0	64(7/11) 31–89 ^a	95 (21/22) 77–99 ^a	85 (28/33) 61–91 ^a
One index or another index			
Visual score ≥ 2 or ADC ≤ 1.08	100 (11/11) 72–100 ^a	73 (16/22) 50–89 ^a	82 (27/33) 65–93 ^a
SUVmax > 3.3 or ADC ≤ 1.08	100 (11/11) 72–100 ^a	86 (19/22) 65–97 ^a	91 (30/33) 76–98 ^a
A/L SUVmax ratio ^b > 1.0 or ADC ≤ 1.08	100 (11/11) 72–100 ^a	86 (19/22) 65–97 ^a	91 (30/33) 76–98 ^a
Visual score ≥ 2 or SUVmax/ADC ratio ^c > 4.0	100 (11/11) 72–100 ^a	73 (16/22) 50–89 ^a	82 (27/33) 65–93 ^a
SUVmax > 3.3 or SUVmax/ADC ratio ^c > 4.0	100 (11/11) 72–100 ^a	86 (19/22) 65–97 ^a	91 (30/33) 76–98 ^a
A/L SUVmax ratio ^b > 1.0 or SUVmax/ADC ratio ^c > 4.0	100 (11/11) 72–100 ^a	86 (19/22) 65–97 ^a	91 (30/33) 76–98 ^a
ADC ≤ 1.08 or SUVmax/ADC ratio ^c > 4.0	81 (9/11) 48–98 ^a	95 (21/22) 77–99 ^a	91 (30/33) 76–98 ^a

SUVmax, maximum standardized uptake value; ADC, apparent diffusion coefficient ($\times 10^{-3}$ mm²/s)

^a 95% confidence interval

^b A/L SUVmax ratio = adrenal lesion-to-liver SUVmax ratio

^c SUVmax/ADC ratio = adrenal lesion SUVmax $\times 10^{-3}$ mm²/s/ADC

Representative images of adrenal adenoma and pheochromocytoma are shown in Figs. 3 and 4, respectively.

Discussion

The purpose of this study was to examine the diagnostic performances of FDG-based indices and DWI ADC to distinguish between benign pheochromocytoma and other benign adrenal tumors in the patients who were performed both FDG-PET/CT and DWI examinations. For this purpose, we selected retrospectively the eligible patients from the MRI database. As a result, the

frequencies of individual incidentalomas differed considerably from those of imaged population [1]; 11 pheochromocytomas (33%) and 22 other benign adrenal tumors (67%) including 17 lipid-poor adenomas (52%), 3 myelolipomas (9%) and 2 schwannomas (6%), all of which might be difficult to be diagnosed by one-point unenhanced CT examinations unless the macroscopic fat component was present in myelolipoma [21].

FDG-PET and PET/CT have been reported to be valuable in the differentiation of adrenal masses, especially between malignant and benign lesions [20]. Although the normal adrenal gland shows uptake of FDG,

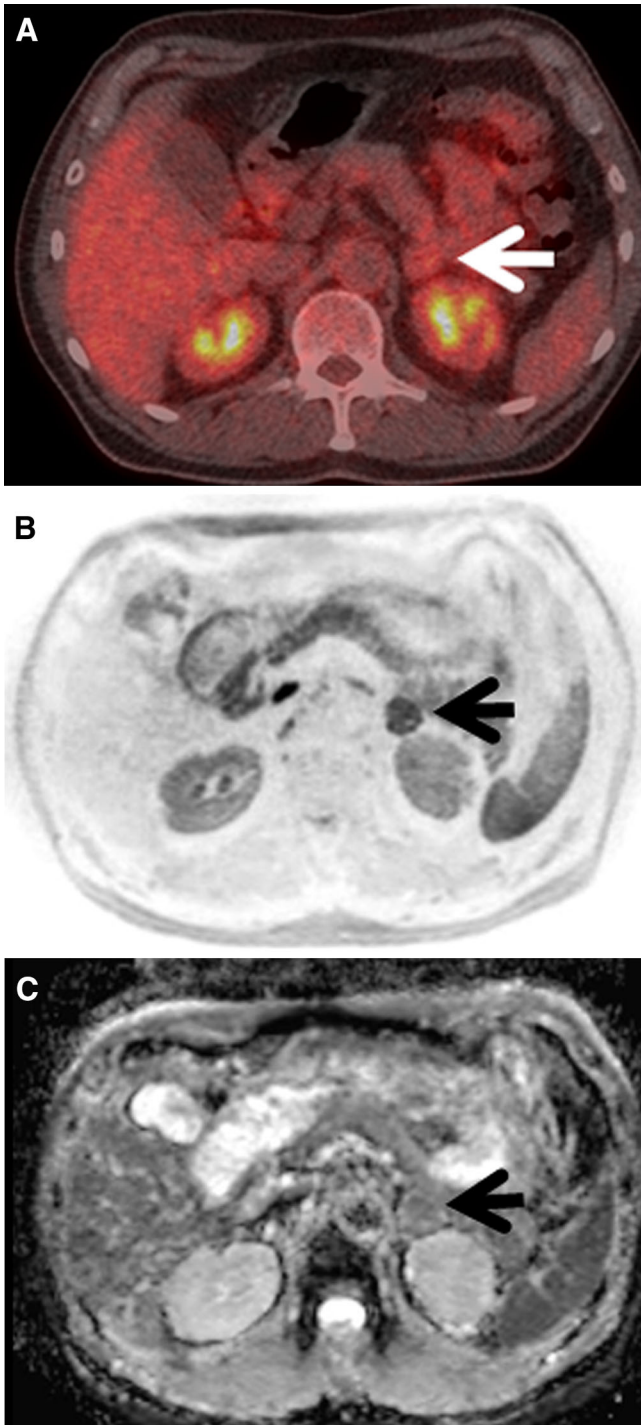


Fig. 3. 62-year-old man with a left adrenal lipid-poor adenoma (Tumor 6). The left adrenal tumor shows slight FDG uptake (arrow) (visual score, 1; SUVmax, 3.3; A/L SUVmax ratio, 0.73) on FDG-PET/CT (A), hyperintensity (arrow) on DWI (B) and a high ADC ($1.23 \times 10^{-3} \text{ mm}^2/\text{s}$, arrow) on the ADC map (C).

SUVmax ranges from 0.95 to 2.46, generally less than that of the liver [22]. Groussin et al. [23] reported that use of a SUVmax cutoff of 3.4 offered a sensitivity of 100% and a specificity of 70% in distinguishing between ade-

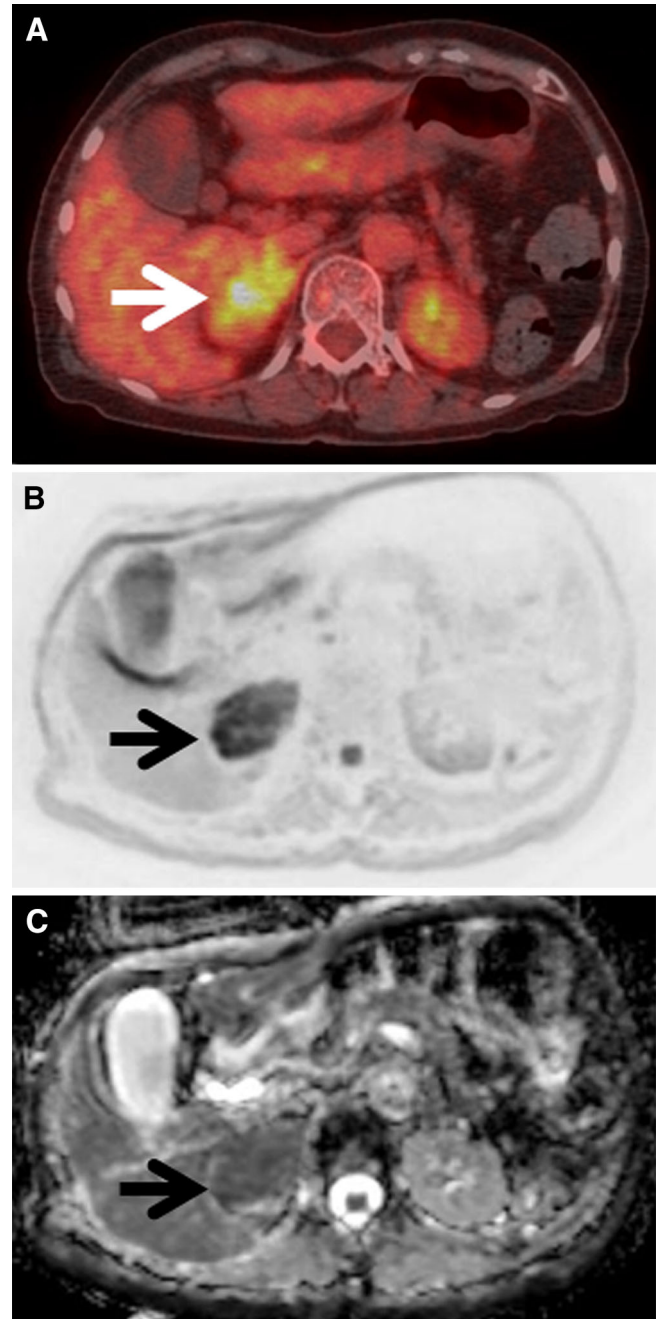


Fig. 4. 72-year-old woman with a right adrenal pheochromocytoma (Tumor 29). The right adrenal tumor shows increased FDG uptake (arrow) (visual score, 3; SUVmax, 6.1, A/L SUVmax ratio, 1.79) on FDG-PET/CT (A), hyperintensity (arrow) on DWI (B) and a lower ADC ($0.95 \times 10^{-3} \text{ mm}^2/\text{s}$, arrow) on the ADC map (C).

noma and adrenocortical carcinoma. Metser et al. [24] reported that use of an SUV cutoff of 3.1 yielded a sensitivity of 100% and a specificity of 98% for diagnosing malignancy. When the SUVmax did not exceed that of the liver (A/L SUVmax ratio < 1), FDG/PET demonstrated a sensitivity of 93.8% and a specificity of 100% for diagnosing benign adrenal tumors [25]. In that

report, the A/L SUVmax ratio ranged between 0.22 and 1.47 for benign lesions.

In the present study, 16 of 22 (73%) benign non-pheochromocytoma tumors showed visually weak FDG uptake (visual score 0–1), and the mean SUVmax and A/L SUVmax ratio for these 22 benign tumors were 3.2 (range 1.9–7.9) and 0.96 (range 0.58–2.59), respectively. Seventeen lipid-poor adenomas showed similar findings (mean SUVmax, 2.7 (range 1.9–3.3); mean A/L SUVmax ratio, 0.78 (range 0.58–1.00), and these results were compatible with those in the reports described above.

Shulkin et al. [11] found FDG-avid pheochromocytomas in 22 of 29 patients (76%). Taïeb et al. [12] investigated 28 patients with benign and malignant chromaffin-derived tumors (pheochromocytoma and paraganglioma) and reported that the mean SUVmax was 8.2 (range 1.9–42) for benign tumors and 9.7 (range 2.3–29.3) for malignant tumors. In our study, all benign pheochromocytomas showed FDG-avid uptake above the liver activity (visual score 2–3), and the mean SUVmax and A/L SUVmax ratio were 11.0 (range 3.8–32.5) and 3.96 (range 1.1–10.8), respectively, significantly higher than those of other benign adrenal tumors. Pheochromocytomas, even benign tumors, may thus show high FDG-avid uptake like malignant adrenal tumors.

To the best of our knowledge, only a few reports have described ADC for pheochromocytoma [18, 19]. Song et al. [18] found no significant difference in mean ADC between benign pheochromocytoma [$n = 22$, 1.15 (range 0.49 – 2.14) $\times 10^{-3}$ mm²/s] and lipid-poor adenoma [$n = 18$, 1.07 (range 0.81 – 1.53) $\times 10^{-3}$ mm²/s] at 3.0 T ($b = 0$ and 800 s/mm²). However, Dong et al. [19] used the same 3.0 T machine ($b = 0$ and 800 s/mm²) found the mean ADC ($n = 29$, $0.918 \pm 0.124 \times 10^{-3}$ mm²/s) of benign pheochromocytoma which was lower than that of Song et al. We found that the mean ADC was significantly lower in pheochromocytoma ($1.08 \pm 0.23 \times 10^{-3}$ mm²/s; range 0.72 – 1.43×10^{-3} mm²/s) than in either other benign adrenal tumors ($1.43 \pm 0.29 \times 10^{-3}$ mm²/s; range 1.10 – 1.99×10^{-3} mm²/s) or lipid-poor adenoma ($1.43 \pm 0.30 \times 10^{-3}$ mm²/s; range 1.10 – 1.99×10^{-3} mm²/s) at the different 3.0 T machine ($b = 0$ and 1000 s/mm²). The reasons for wide variation of ADC values between the studies are not clear. However, they may be related to differences in used machines, imaging parameters including b values and the number of tumors.

Although the diagnostic accuracies to differentiate pheochromocytoma from other benign adrenal tumors did not differ significantly between individual FDG-based indices and ADC, the sensitivity and specificity differed between FDG-based indices and ADC: On FDG-PET/CT, the sensitivities were high (100% for all FDG-based indices [11/11]), but the specificities were low; 73% (16/22) for visual score, 86% (19/22) for SUVmax and A/L ratio, respectively. The false-positive non-pheochromocytoma tumors were 3 adenomas, 2

schwannomas and one myelolipoma for visual score, and 2 schwannomas and one myelolipoma for SUVmax and A/L ratio. It is known that occasionally, adenomas demonstrate positive FDG uptake, at levels even those in the liver [2]. However, 3 false-positive adenomas with visual score 2 showed SUVmax of 2.9–3.2 and A/L ratio of 0.97–1.0 which were less than the individual cutoff values. Thus, 2 schwannomas and one myelolipoma were definitively false positive. Although FDG uptake was reported to be low in 6 myelolipomas [24], high uptake of FDG was also noted in 3 myelolipomas [26, 27] and in a schwannoma [28] as case reports, respectively. These results suggest that some benign non-pheochromocytoma adrenal tumors (27% for visual score and 14% for SUVmax and A/L ratio in our study) can show avid FDG uptake like pheochromocytoma.

On the other hand, on MRI, the specificity was high, 100% (22/22), and the sensitivity was low, 64% (7/11) due to 4 false-negative pheochromocytomas for ADC, suggesting that some pheochromocytomas (36% in our study) can exhibit ADC values like non-pheochromocytoma tumors. The reasons why some pheochromocytomas showed the high ADC values like non-pheochromocytoma tumors are unknown. However, 3 of 4 false-negative pheochromocytomas showed relatively low FDG uptake (SUVmax; 3.8, 4, and 5.1) in comparison with 7 other pheochromocytomas (SUVmax; 6–18.9). Thus, metabolic activity may be related to ADC.

When we examined the relationship between FDG SUVmax and ADC for all tumors, a significant negative correlation was identified between SUVmax and ADC (Fig. 2). Given the higher SUVmax in pheochromocytomas compared to other benign adrenal tumors, these results appear to agree with previous reports of a significant negative correlation between SUVmax and ADC in breast cancers and head and neck cancers [29, 30]. FDG uptake in the tumor represents glycolytic activity, which is influenced by several enzymatic and biological properties [31], while ADC reflects the restriction of water molecular diffusivity by microstructural barriers in biological tissues such as cell membranes [32]. The moderate negative correlation between SUVmax and ADC revealed in the present study suggests that glycolytic activity shows a significant relationship to the microstructural environment in adrenal tumors. Thus, we generated a new index using this negative correlation, SUVmax/ADC ratio. Although this index and other indices did not differ significantly in diagnostic accuracy, it yielded the highest AUC of 0.97, the balanced sensitivity (82% [9/11]), specificity (95% [21/22]), positive predictive value (90% [9/10]), and negative predictive value (91% [21/23]).

We examined whether combination of two of each modality indices could improve the diagnostic accuracy. However, the significant improvement in diagnostic accuracy was not obtained in any combinations

(Table 3). This may be due to the relatively high diagnostic accuracy of each index in this small study population. Apart from the diagnostic accuracy, the confident level would increase when concordant results are obtained in various indices.

¹²³I-MIBG, a noradrenaline analog, accumulates in pheochromocytomas. Previous reports have shown that ¹²³I-MIBG imaging offers a sensitivity of 83–100% and a specificity of 95–100% for diagnosing pheochromocytomas [8]. In the present study, no false-negative or false-positive tumors were identified among 11 pheochromocytomas and 17 non-pheochromocytoma tumors of the 25 patients who underwent ¹²³I-MIBG imaging. Although ¹²³I-MIBG imaging showed the highest sensitivity and specificity, both FDG-based indices and ADC also showed high accuracies in discriminating between pheochromocytoma and other benign adrenal tumors (Table 2). Some reports have described false-negative MIBG examinations that might have been caused by necrosis or dedifferentiation of pheochromocytomas [33], and FDG-PET/CT may help diagnose pheochromocytoma in such cases, as described by Mamede et al. [34].

Boland et al. suggested an excellent algorithmic approach including biochemical assessment, previous imaging, various CT, MRI, and PET methods, and biopsy in characterization of adrenal incidentalomas [1]. Biochemical assessment is essential for characterization of adrenal incidentalomas, and when pheochromocytoma is suspected biochemically, MIBG imaging may be the first choice of morphological imaging methods. However, biochemical examinations are not always performed before detailed morphological evaluation using contrast enhanced CT, MRI, and FDG-PET/CT in clinical practice. When adrenal incidentalomas are discovered, FDG-based indices or ADC may be useful as well as other morphological methods to differentiate pheochromocytoma from other benign adrenal tumors.

Various limitations of this retrospective study should be considered when interpreting the results. As already mentioned, the resultant study cohort was biased and selected. The study included a relatively small number of patients from a single institution. Pathological confirmation was not always obtained for all tumors. Intervals between FDG-PET/CT and MRI varied substantially (range 3–71 days), and most patients were done FDG-PET/CT first. Therefore, an incidental finding of FDG-PET/CT might lead to MRI which led to biased population. No lipid-rich adenomas were identified in the resultant study population, probably because lipid-rich adenomas were diagnosed by their low density on unenhanced CT, and further imaging studies were considered unnecessary [1]. Tumors less than 1 cm in diameter were not identified, probably because of the limited resolution of PET [2]. Comparison between benign and malignant tumors was not performed. We speculate that discriminating pheochromocytoma from malignant

adrenal tumors by FDG indices or ADC might be difficult, because our study revealed that pheochromocytoma typically shows high FDG uptake and low ADC, which may be similar to malignant adrenal tumors. However, this speculation remains to be clarified.

In conclusion, although ¹²³I-MIBG imaging may be a specific imaging modality for diagnosing pheochromocytoma, FDG indices and ADC may also prove highly diagnostic in differentiating pheochromocytoma from other benign adrenal tumors.

References

1. Boland GW, Blake MA, Hahn PF, Mayo-Smith WW (2008) Incidental adrenal lesions: principles, techniques, and algorithms for imaging characterization. *Radiology* 249:756–775
2. Chong S, Lee Ks, Kim HY, et al. (2006) Integrated PET-CT for the characterization of adrenal gland lesions in cancer patients: diagnostic efficacy and interpretation pitfalls. *Radiographics* 26:1811–24
3. Caoili EM, Korobkin M, Francis IR, Cohan RH, Dunnick NR (2000) Delayed enhanced CT of lipid-poor adrenal adenomas. *AJR Am J Roentgenol* 175:1411–1415
4. Boland GW, Lee MJ, Gazelle GS, et al. (1998) Characterization of adrenal masses using unenhanced CT: an analysis of the CT literature. *AJR Am J Roentgenol* 171:201–204
5. Szolar DH, Korobkin M, Reittner P, et al. (2005) Adrenocortical carcinomas and adrenal pheochromocytomas: mass and enhancement loss evaluation at delayed contrast-enhanced CT. *Radiology* 234:479–485
6. Park BK, Kim CK, Kwon GY, Kim JH (2007) Re-evaluation of pheochromocytomas on delayed contrast-enhanced CT: washout enhancement and other imaging features. *Eur Radiol* 17:2804–2809
7. Fujiyoshi F, Nakajo M, Fukukura Y, Tsuchimochi S (2003) Characterization of adrenal tumors by chemical shift low-angle shot MR imaging: comparison of four methods of quantitative evaluation. *AJR Am J Roentgenol* 180:1649–1657
8. Havekes B, King K, Lai EW, et al. (2010) New imaging approaches to pheochromocytomas and paragangliomas. *Clin Endocrinol (Oxf)* 72:137–145
9. von Schulthess GK, Steinert HC, Hany TF (2006) Integrated PET/CT: Current applications and future directions. *Radiology* 238:405–422
10. Wong KK, Arabi M, Zerizer I, et al. (2011) Role of positron emission tomography/computed tomography in adrenal and neuroendocrine tumors: fluorodeoxyglucose and nonfluorodeoxyglucose tracers. *Nucl Med Commun* 32:764–781
11. Shulkin BL, Thompson NW, Shapiro B, Francis IR, Sisson JC (1999) Pheochromocytomas: imaging with 2-[Fluorine-18] fluoro-2-deoxy-D-glucose PET. *Radiology* 212:35–41
12. Taïeb D, Sebag F, Barlier A, et al. (2009) 18F-FDG avidity of pheochromocytomas and paragangliomas: a new molecular imaging signature? *J Nucl Med* 50:711–717
13. Koh DM, Collins DJ (2007) Diffusion-weighted MRI in the body: applications and challenges in oncology. *AJR Am J Roentgenol* 188:1622–1635
14. Tsushima Y, Takahashi-Taketomi A, Endo K (2009) Diagnostic utility of diffusion-weighted imaging and apparent diffusion coefficient for the diagnosis of adrenal tumors. *J Magn Reson Imaging* 29:112–117
15. Miller F, Wang Y, McCarthy RJ, et al. (2010) Utility of diffusion-weighted MRI in characterization of adrenal lesions. *AJR Am J Roentgenol* 194:W179–W185
16. Halefoglu AM, Altun I, Disli C, et al. (2012) A prospective study on the utility of diffusion-weighted quantitative chemical-shift magnetic resonance imaging in the distinction of adrenal adenomas and metastases. *J Comput Assist Tomogr* 36:367–374
17. Sandrasegaran K, Patel AA, Ramaswamy R, et al. (2011) Characterization of adrenal masses with diffusion-weighted imaging. *AJR Am J Roentgenol* 197:132–138

18. Song J, Zhang C, Liu Q, et al. (2012) Utility of chemical shift and diffusion-weighted imaging in characterization of hyperattenuating adrenal lesions at 3.0T. *Eur J Radiol* 81:2137–2143
19. Dong Y, Liu Q (2012) Differentiation of malignant from benign pheochromocytomas with diffusion-weighted and dynamic contrast-enhanced magnetic resonance at 3.0T. *J Comput Assist Tomogr* 36:361–366
20. Boland GW, Blake MA, Holalkere NS, Hahn PF (2009) PET/CT for the characterization of adrenal masses in patients with cancer: qualitative vs. quantitative accuracy in 150 consecutive patients. *AJR Am J Roentgenol* 192:956–962
21. Low G, Dhliwayo H, Lomas DJ (2012) Adrenal neoplasms. *Clin Radiol* 67:988–1000
22. Bagheri B, Maurer AH, Cone L, Doss M, Adler L (2004) Characterization of the normal adrenal gland with ¹⁸F-FDG PET/CT. *J Nucl Med* 45:1340–1343
23. Groussin L, Bonardel G, Silvéra S, et al. (2009) ¹⁸F-Fluorodeoxyglucose positron emission tomography for the diagnosis of adrenocortical tumors: a prospective study in 77 operated patients. *J Clin Endocrinol Metab* 94:1713–1722
24. Metser U, Miller E, Lerman H, et al. (2006) ¹⁸F-FDG PET/CT in the evaluation of adrenal masses. *J Nucl Med* 47:32–37
25. Blake MA, Slattery JM, Kalra MK, et al. (2006) Adrenal lesions: characterization with fused PET/CT image in patients with proved or suspected malignancy-initial experience. *Radiology* 238:970–977
26. Castinetti F, Verschueren A, Cassagneau P, et al. (2012) Adrenal myelolipoma: an unusual cause of bilateral highly ¹⁸F-FDG-avid adrenal masses. *J Clin Endocrinol Metab* 97:2577–2578
27. Ludwig V, Rice MH, Martin WH, Kelley MC, Delbeke D (2002) 2-Deoxy-2-[¹⁸F]fluoro-D-glucose positron emission tomography uptake in a giant adrenal myelolipoma. *Mol Imaging Biol* 4:355–358
28. Adas S, Ozullker F, Adas G, et al. (2013) A rare adrenal incidentaloma: adrenal schwannoma. *Case Rep Gastroenterol* 7:420–427
29. Nakajo M, Kajiya Y, Kaneko T, et al. (2010) FDG PET/CT and diffusion-weighted imaging for breast cancer: prognostic values of maximum standardized uptake values and apparent diffusion coefficient values of the primary lesion. *Eur J Nucl Med Mol Imaging* 37:2011–2020
30. Nakajo M, Nakajo M, Kajiya Y, et al. (2012) FDG PET/CT and diffusion-weighted imaging of head and neck squamous cell carcinoma: comparison of prognostic significance between primary tumor standardized uptake value and apparent diffusion coefficient. *Clin Nucl Med* 37:475–480
31. Rigo P, Paulus P, Kaschten BJ, et al. (1996) Oncological applications of positron emission tomography with fluorine-18 fluorodeoxyglucose. *Eur J Nucl Med* 23:1641–1674
32. Sinha S, Lucas-Quesada FA, Sinha U, DeBruhl N, Bassett LW (2002) In vivo diffusion-weighted MRI of the breast: potential for lesion characterization. *J Magn Reson Imaging* 15:693–704
33. Ilias I, Sahdev A, Reznick RH, Grossman AB, Pacak K (2007) The optimal imaging of adrenal tumours: a comparison of different methods. *Endocr Relat Cancer* 14:587–599
34. Mamede M, Carrasquillo JA, Chen CC, et al. (2006) Discordant localization of 2-[¹⁸F]-fluoro-2-deoxy-D-glucose in 6-[¹⁸F]-fluoro-dopamine- and [(123)I]-metaiodobenzylguanidine-negative metastatic pheochromocytoma sites. *Nucl Med Commun* 27:31–36